

Exotic flavor states in the hidden gauge formalism

R. Molina, T. Branz, N. Ikeno, L.R. Dai and E. Oset



Table of contents

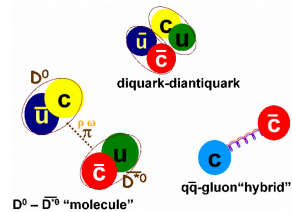
1. Introduction
2. The Local Hidden Gauge Approach
3. The $X_0(2866)$ and its spin partners
4. Doubly-charmed states
5. Z_{cs} states
6. Conclusions

Intro

Introduction

Since the X(3872) many exotics discovered ...

- $Z_c(3900)$, BESIII, 2013
close to $D\bar{D}^*$, $c\bar{q}q\bar{c}$ ($q = u, d$)
- $Z_{cs}(3985)$, BESIII, 2021
close to $\bar{D}_s^* D / \bar{D}_s D^*$, $c\bar{q}s\bar{c}$
- $X_0(2866), X_1(2900)$, LHCb, 2020
close to $D^*\bar{K}^*$, $c\bar{q}s\bar{q}$
- $T_{cc}(3875)$, LHCb, 2021
close to DD^* , $c\bar{q}c\bar{q}$
- $T_{cs}(2900)$ LHCb, 2022, $c\bar{s}q\bar{q}$



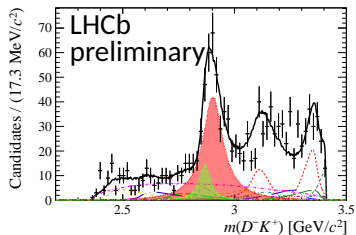
⇒ Do not fit into $q\bar{q}$ basic mesons of the quark model predictions
... Are the meson-meson molecules? tetraquarks?
... Dynamics of the interaction?

New flavor exotic tetraquark ($C = -1; S = 1$)

LHCb (2020)

Two states $J^P = 0^+, 1^-$ decaying to $\bar{D}K$. First clear example of an heavy-flavor exotic tetraquark, $\sim \bar{c}\bar{s}ud$.

$X_0(2866) : M = 2866 \pm 7$ and $\Gamma = 57.2 \pm 12.9 \text{ MeV}$,
 $X_1(2900) : M = 2904 \pm 5$ and $\Gamma = 110.3 \pm 11.5 \text{ MeV}$.



R. Aaij et al. (LHCb Collaboration), PRL125(2020), PRD102(2020)

Flavour exotic states

- 2010. Prediction of several flavour exotic states

PHYSICAL REVIEW D 82, 014010 (2010)

New interpretation for the $D_{s2}^*(2573)$ and the prediction of novel exotic charmed mesons

R. Molina,¹ T. Branz,² and E. Oset¹

¹Departamento de Física Teórica and IFIC, Centro Mixto Universidad de Valencia-CSIC, Institutos de Investigación de Paterna, Apartado 22085, 46071 Valencia, Spain

²Institut für Theoretische Physik, Universität Tübingen, Kepler Center for Astro and Particle Physics, Auf der Morgenstelle 14, D-72076 Tübingen, Germany

(Received 4 May 2010; published 21 July 2010)

In this manuscript we study the vector-vector interaction within the hidden-gauge formalism in a coupled channel unitary approach. In the sector $C = 1, S = 1, J = 2$ we get a pole in the T matrix around 2572 MeV that we identify with the $D_{s2}^*(2573)$, coupling strongly to the $D^*K^*(D_s^*\phi(\omega))$ channels. In addition we obtain resonances in other exotic sectors which have not been studied before such as $C = 1, S = -1, C = 2, S = 0$ and $C = 2, S = 1$. These “flavor-exotic” states are interpreted as D^*K^* , D^*D^* and D^*D^* molecular states but have not been observed yet. In total we obtain nine states with different spin, isospin, charm, and strangeness of non- $C = 0, S = 0$ and $C = 1, S = 0$ character, which have been reported before.

DOI: 10.1103/PhysRevD.82.014010

PACS numbers: 14.40.Rt, 12.40.Vv, 13.75.Lb, 14.40.Lb

- Free parameter fixed with $D_{s2}(2573)$; couples to D^*K^* , $c\bar{q}q\bar{s}$
- Flavour exotic states with $I = 0, J^P = \{0, 1, 2\}^+$ coupling to $D^*\bar{K}^*$ are predicted, $c\bar{q}s\bar{q}$
- Doubly charm states, $I = 0; J^P = 1^+$, close to D^*D^* are predicted, $c\bar{q}c\bar{q}$, and $I = 1/2; J^P = 1^+$, close to $D^*D_s^*$ $c\bar{q}c\bar{s}$

Flavour exotic states

Molina, Branz, Oset, PRD82(2010)

C, S	Channels	$I[J^P]$	\sqrt{s}	$\Gamma_A(\Lambda = 1400)$	$\Gamma_B(\Lambda = 1200)$	State	\sqrt{s}_{exp}	Γ_{exp}
1, -1	$D^* \bar{K}^*$	0[0 ⁺]	2848	23	59	$X_0(2866)$	2866	57
		0[1 ⁺]	2839	3	3	How to observe the $J^P = 1^+$?		
		0[2 ⁺]	2733	11	36	For $J^P = 2^+$ see Eulogio's talk		
1, 1	$D^* K^*, D_s^* \omega$ $D_s^* \phi$	0[0 ⁺]	2683	20	71			
		0[1 ⁺]	2707	4×10^{-3}	4×10^{-3}			
		0[2 ⁺]	2572	7	23	$D_{s2}(2573)$	2572.6 ± 0.9	20 ± 5
1, 1	$D^* K^*, D_s^* \rho$	1[2 ⁺]	2786	8	11			
2, 0	$D^* D^*$	0[1 ⁺]	3969	0	0			
2, 1	$D^* D_s^*$	1/2[1 ⁺]	4101	0	0			

Table 1: Summary of the nine states obtained. The width is given for the model A, Γ_A , and B, Γ_B . All the quantities here are in MeV. Repulsion in $C = 0, S = 1, I = 1/2$; $C = 1, S = -1, I = 1$; $C = 1, S = 2, I = 1/2$; $C = 2, S = 0, I = 1$ and $C = 2, S = 2, I = 0$ is found.

Form factors in the $D^* D\pi$ vertex; Model A: $F_1(q^2) = \frac{\Lambda_b^2 - m_\pi^2}{\Lambda_b^2 - q^2}$, Titov, Kampfer EPJA7, PRC65 with $\Lambda_b = 1.4, 1.5$ GeV and

$g = M_\rho / 2 f_\pi$. Model B: $F_2(q^2) = e^{q^2/\Lambda^2}$ Navarra, Nielsen, Bracco PRD65 (2002), $\Lambda = 1, 1.2$ GeV and $g_D = g_{D^* D\pi}^{\text{exp}} = 8.95$ (experimental value). Subtraction constant $\alpha = -1.6$.

Many studies appeared after these discoveries ...

- He, Wang, Zhu, EPJC80, 1026 (2020), Karliner, Rosner, PRD102(2020), $X_0(2866)$, compact tetraquark
- X. H. Liu, Yan et al., EPJC80(2020), $X_0(2866)$, Triangle Singularity
- M. Z. Liu, Xie, Geng, PRD102(2020), $X_0(2866)$, $D^* \bar{K}^*$ molecule (one-boson ex.), $X_1(2900)$ cannot be, Qi, Wang et al. EPJC81(2021), X_1 is a $\bar{D}_1 K$ molecule (ρ , ω ex.)
- Ge, X. H. Liu, EPJC81(2021), $Z_{cs}(4000)$, $X(4700)$, threshold effects
- Du, Albaladejo, F. K. Guo, Nieves, PRD105(2022), energy dep. interaction, $Z_{cs}(3985)$ and $Z_c(3900)$ are SU(3) partners, $D^* \bar{D}_{(s)} / D \bar{D}_{(s)}^*$
- Du, Baru, Dong, Filin, Nieves, F. K. Guo, T_{cc} , PRD105, (2022), 3-body dynamics, $D^0 D^0 \pi^+$, contact+OPE, DD^* molecule
- Albaladejo, T_{cc} from DD^* , can have $I = 0$ or 1
- Feijoo, Liang, Oset, PRD104(2021), T_{cc} as DD^* , has $I = 0$, decay width to $D^0 D^0 \pi^+ \sim 43$ MeV
- Padmanath, Prelovsek, PRL 129 (2022) virtual s-wave bound state for $m_\pi = 280$ MeV of DD^* in LatticeQCD ...

The Local Hidden Gauge Approach

The hidden gauge formalism Bando,Kugo,Yamawaki

Lagrangian

$$\mathcal{L} = \mathcal{L}^{(2)} + \mathcal{L}_{III} \quad (1)$$

$$\mathcal{L}^{(2)} = \frac{1}{4} f^2 \langle D_\mu U D^\mu U^\dagger + \chi U^\dagger + \chi^\dagger U \rangle \quad (2)$$

$$\mathcal{L}_{III} = -\frac{1}{4} \langle V_{\mu\nu} V^{\mu\nu} \rangle + \frac{1}{2} M_V^2 \langle [V_\mu - \frac{i}{g} \Gamma_\mu]^2 \rangle$$

$$D_\mu U = \partial_\mu U - ieQA_\mu U + ieUQA_\mu, \quad U = e^{i\sqrt{2}P/f} \quad (3)$$

$$\begin{aligned} \mathcal{L}_{V\gamma} &= -M_V^2 \frac{e}{g} A_\mu \langle V^\mu Q \rangle \\ \mathcal{L}_{VPP} &= -ig \langle V^\mu [P, \partial_\mu P] \rangle; \quad g = M_V/2f \\ \widetilde{\mathcal{L}}^{(2)} &= \frac{1}{12f^2} \langle [P, \partial_\mu P]^2 + MP^4 \rangle. \end{aligned} \quad (4)$$

Local Hidden Gauge Approach

Vector-vector scattering

$$\mathcal{L}_{III} = -\frac{1}{4} \langle V_{\mu\nu} V^{\mu\nu} \rangle$$

$$\mathcal{L}_{III}^{(3V)} = ig \langle (\partial_\mu V_\nu - \partial_\nu V_\mu) V^\mu V^\nu \rangle$$

$$\mathcal{L}_{III}^{(c)} = \frac{g^2}{2} \langle V_\mu V_\nu V^\mu V^\nu - V_\nu V_\mu V^\mu V^\nu \rangle$$

$$V_{\mu\nu} =$$

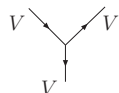
$$\partial_\mu V_\nu - \partial_\nu V_\mu - ig[V_\mu, V_\nu]$$

$$g = \frac{M_V}{2f}$$

$$V_\mu = \begin{pmatrix} \frac{\rho^0}{\sqrt{2}} + \frac{\omega}{\sqrt{2}} & \rho^+ & K^{*+} & \bar{D}^{*0} \\ \rho^- & -\frac{\rho^0}{\sqrt{2}} + \frac{\omega}{\sqrt{2}} & K^{*0} & D^{*-} \\ K^{*-} & \bar{K}^{*0} & \phi & D_s^{*-} \\ D^{*0} & D^{*+} & D_s^{*+} & J/\psi \end{pmatrix}_\mu$$



a)



b)

→



c)



d)

Local Hidden Gauge Approach

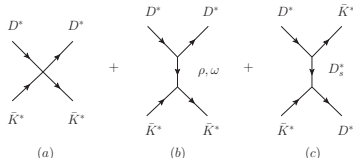


Figure 1: The $D^* \bar{K}^* \rightarrow D^* \bar{K}^*$ interaction at the tree level; (a) contact term; (b) exchange of light vectors; (c) exchange of a heavy vector.

Approximation

$$\epsilon_1^\mu = (0, 1, 0, 0)$$

$$\epsilon_2^\mu = (0, 0, 1, 0)$$

$$\epsilon_3^\mu = (|\vec{k}|, 0, 0, k^0)/m$$

$$k^\mu = (k^0, 0, 0, |\vec{k}|)$$

$$\vec{k}/m \simeq 0, k_j^\mu \epsilon_\mu^{(I)} \simeq 0$$

$$\epsilon_1^\mu = (0, 1, 0, 0)$$

$$\epsilon_2^\mu = (0, 0, 1, 0)$$

$$\epsilon_3^\mu = (0, 0, 0, 1)$$

$$\mathcal{L}_{III}^{(3V)} = ig \langle (\partial_\mu V_\nu - \partial_\nu V_\mu) V^\mu V^\nu \rangle = ig \langle [V_\mu, \partial_\nu V_\mu] V^\nu \rangle$$

Spin projectors

$$\mathcal{P}^{(0)} = \frac{1}{3} \epsilon_\mu \epsilon^\mu \epsilon_\nu \epsilon^\nu; \quad \mathcal{P}^{(1)} = \frac{1}{2} (\epsilon_\mu \epsilon_\nu \epsilon^\mu \epsilon^\nu - \epsilon_\mu \epsilon_\nu \epsilon^\nu \epsilon^\mu)$$

$$\mathcal{P}^{(2)} = \left\{ \frac{1}{2} (\epsilon_\mu \epsilon_\nu \epsilon^\mu \epsilon^\nu + \epsilon_\mu \epsilon_\nu \epsilon^\nu \epsilon^\mu) - \frac{1}{3} \epsilon_\mu \epsilon^\mu \epsilon_\nu \epsilon^\nu \right\}.$$

The $X_0(2866)$ and its spin partners

Local Hidden Gauge Approach

Potential V : contact + vector-meson exchange (ρ, ω)

J	Amplitude	Contact	V-exchange	\sim Total
0	$D^* \bar{K}^* \rightarrow D^* \bar{K}^*$	$4g^2 - \frac{g^2(p_1+p_4) \cdot (p_2+p_3)}{m_{D_s^*}^2} + \frac{1}{2}g^2(\frac{1}{m_\omega^2} - \frac{3}{m_\rho^2})(p_1+p_3) \cdot (p_2+p_4)$		$-9.9g^2$
1	$D^* \bar{K}^* \rightarrow D^* \bar{K}^*$	$0 + \frac{g^2(p_1+p_4) \cdot (p_2+p_3)}{m_{D_s^*}^2} + \frac{1}{2}g^2(\frac{1}{m_\omega^2} - \frac{3}{m_\rho^2})(p_1+p_3) \cdot (p_2+p_4)$		$-10.2g^2$
2	$D^* \bar{K}^* \rightarrow D^* \bar{K}^*$	$-2g^2 - \frac{g^2(p_1+p_4) \cdot (p_2+p_3)}{m_{D_s^*}^2} + \frac{1}{2}g^2(\frac{1}{m_\omega^2} - \frac{3}{m_\rho^2})(p_1+p_3) \cdot (p_2+p_4)$		$-15.9g^2$

Table 2: Tree level amplitudes for $D^* \bar{K}^*$ in $I = 0$. Last column: ($V_{\text{th.}}$).

J	Amplitude	Contact	V-exchange	\sim Total
0	$D^* \bar{K}^* \rightarrow D^* \bar{K}^*$	$-4g^2 + \frac{g^2(p_1+p_4) \cdot (p_2+p_3)}{m_{D_s^*}^2} + \frac{1}{2}g^2(\frac{1}{m_\omega^2} + \frac{1}{m_\rho^2})(p_1+p_3) \cdot (p_2+p_4)$		$9.7g^2$
1	$D^* \bar{K}^* \rightarrow D^* \bar{K}^*$	$0 - \frac{g^2(p_1+p_4) \cdot (p_2+p_3)}{m_{D_s^*}^2} + \frac{1}{2}g^2(\frac{1}{m_\omega^2} + \frac{1}{m_\rho^2})(p_1+p_3) \cdot (p_2+p_4)$		$9.9g^2$
2	$D^* \bar{K}^* \rightarrow D^* \bar{K}^*$	$2g^2 + \frac{g^2(p_1+p_4) \cdot (p_2+p_3)}{m_{D_s^*}^2} + \frac{1}{2}g^2(\frac{1}{m_\omega^2} + \frac{1}{m_\rho^2})(p_1+p_3) \cdot (p_2+p_4)$		$15.7g^2$

Table 3: Tree level amplitudes for $D^* \bar{K}^*$ in $I = 1$. Last column: ($V_{\text{th.}}$).

The interaction is attractive for $I = 0$ and repulsive for $I = 1$.

New flavor exotic tetraquark ($C = 1, S = -1$)

Two-meson loop function

$$G_i(s) = \frac{1}{16\pi^2} \left(\alpha + \text{Log} \frac{M_1^2}{\mu^2} + \frac{M_2^2 - M_1^2 + s}{2s} \text{Log} \frac{M_2^2}{M_1^2} \right. \\ \left. + \frac{p}{\sqrt{s}} \left(\text{Log} \frac{s - M_2^2 + M_1^2 + 2p\sqrt{s}}{-s + M_2^2 - M_1^2 + 2p\sqrt{s}} + \text{Log} \frac{s + M_2^2 - M_1^2 + 2p\sqrt{s}}{-s - M_2^2 + M_1^2 + 2p\sqrt{s}} \right) \right),$$

Bethe-Salpeter

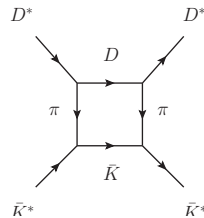
$$T = [\hat{1} - VG]^{-1}V$$

The states with $J^P = \{0, 2\}^+$ decay into $D\bar{K}$

$$\mathcal{L}_{VPP} = -ig \langle [P, \partial_\mu P] V^\mu \rangle$$

$$F(q) = e^{((p_1^0 - q^0)^2 - \vec{q}^2)/\Lambda^2} \quad \text{Navarra, PRD65(2002)}$$

with $q_0 = (s + m_D^2 - m_K^2)/2\sqrt{s}$.



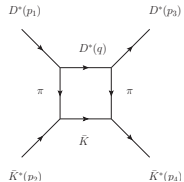
New flavor exotic tetraquark ($C = 1, S = -1$)

Recent work: Molina, Oset PLB811 2020, $\alpha = -1.474$, $\Lambda = 1300$.

Evaluation of the decay width of the $J^P = 1^+$ state

$$\mathcal{L} = \frac{iG'}{\sqrt{2}} \epsilon^{\mu\nu\alpha\beta} \langle \delta_\mu V_\nu \delta_\alpha V_\beta P \rangle$$

$$\mathcal{L}_{VPP} = -ig \langle [P, \partial_\mu P] V^\mu \rangle$$



Combination of the spin projectors, $5\mathcal{P}^{(1)} + 3\mathcal{P}^{(2)}$, zero component for $J = 0$ (violates parity). The imaginary part for $J = 1$ is,

$$\text{Im}t = -\frac{3}{2} \frac{1}{8\pi} (G' g m_{D^*})^2 q^5 \left(\frac{1}{(m_D^* - \omega^*(q))^2 - \omega^2(q)} \right)^2 \frac{1}{\sqrt{s}} F^4(q)$$

$$\omega(q) = \sqrt{m_K^2 + \vec{q}^2}; \omega^*(q) = \sqrt{m_{D^*}^2 + \vec{q}^2}; q = \frac{\lambda^{1/2}(s, m_{D^*}^2, m_K^2)}{2\sqrt{2}}$$

Decay of the $X_0(2900)$ to $D^* \bar{K}$

$I(J^P)$	$M[\text{MeV}]$	$\Gamma[\text{MeV}]$	Coupled channels	state
$0(2^+)$	2775	38	$D^* \bar{K}^*$?
$0(1^+)$	2861	20	$D^* \bar{K}^*$?
$0(0^+)$	2866	57	$D^* \bar{K}^*$	$X_0(2866)$

Table 4: New results including the width of the $D^* K$ channel.

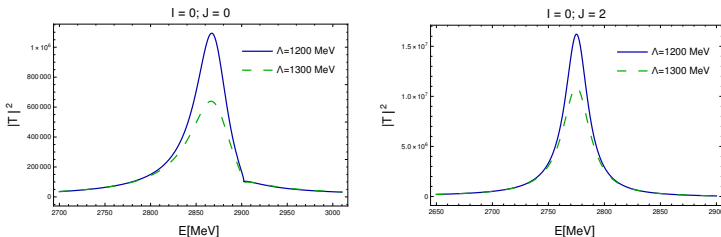


Figure 2: $|T|^2$ for $C = 1, S = -1, I = 0, J = 0$ and $J = 2$.

Decay of the $X_0(2900)$ to $D^* \bar{K}$

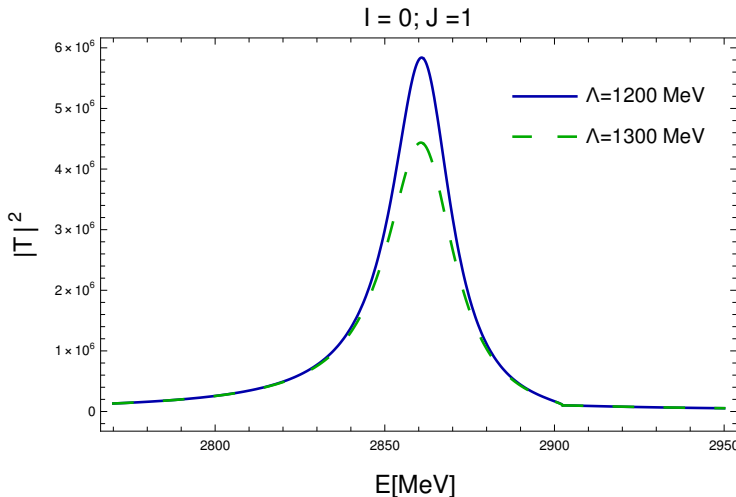


Figure 3: $|T|^2$ for $C = 1, S = -1, I = 0, J = 0$ and $J = 1$.

How can we observe the $J^P = 1^+$ state?

Amo Sanchez et al. (BABAR), PRD83(2011).

The $\bar{B}^0 \rightarrow D^{*+} \bar{D}^{*0} K^-$ reaction:

- It proceeds via external emission (favoring the decay)
- It has the largest branching fraction (1.06%)
- It can produce the $D^{*+} K^-$ in $I = 0$ (decay mode of the 1^+ state).

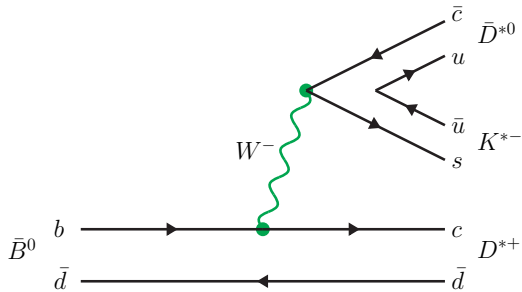


Figure 4: Diagrammatic decay of the $\bar{B}^0 \rightarrow \bar{D}^{*0} D^{*+} K^{*-}$ at the quark level.

How can we observe the $J^P = 1^+$ state?

Hadronization + decay

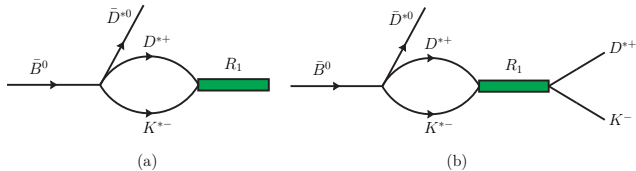


Figure 5: (a) Rescattering of $D^{*+}K^{*-}$ to give the resonance R_1 of $I = 0, J^P = 1^+$; (b) Further decay of R_1 to $D^{*+}K^-$.

$$|D^* \bar{K}^*; I = 0\rangle = -\frac{1}{\sqrt{2}}(D^{*+}K^{*-} + D^{*0}\bar{K}^{*0}). \quad (5)$$

$\bar{B}^0 \rightarrow \bar{D}^{*0} D^{*+} K^{*-}$ vertex: (1) \bar{D}^{*0} , (2) D^{*+} , (3) K^{*-}

$$(s-wave) - i t = -i C \epsilon^{(1)} \cdot (\epsilon^{(2)} \times \epsilon^{(3)}) = -i C \epsilon_{ijk} \epsilon_i^{(1)} \epsilon_j^{(2)} \epsilon_k^{(3)}$$

$$R_I \rightarrow VV \text{ vertex: } -\frac{1}{\sqrt{2}} g_{R,D^*\bar{K}^*} \mathcal{P}^{(J=1)}; \quad \mathcal{P}^{(J=1)} = \frac{1}{2}(\epsilon_i^{(2)} \epsilon_j^{(3)} - \epsilon_j^{(2)} \epsilon_i^{(3)}) \quad 17$$

How can we observe the $J^P = 1^+$ state?

$$\sum_{pol} \epsilon_i^{(1)} \epsilon_{ii'j'}^{(1)} \epsilon_m^{(1)} \epsilon_{mi'j'} = \epsilon_{ii'j'} \epsilon_{ii'j'} = \delta_{ii'} \delta_{jj'} - \delta_{i'j'} \delta_{j'i'} = 9 - 3 = 6$$

$$\sum_{pol} |t'|^2 = \frac{6}{4} C^2 |g_{R_1, D^* \bar{K}^*}|^2 |G_{D^* \bar{K}^*}(M_{\text{inv}})|^2 |g_{R_1, D^* \bar{K}}|^2 \left| \frac{1}{M_{\text{inv}}^2(R_1) - M_{R_1}^2 + iM_{R_1}\Gamma_{R_1}} \right|^2$$

with $M_{\text{inv}}^2 = (P_{D^{*+}} + P_{K^-})^2$. The effective $|g_{R_1, D^* \bar{K}}|^2$ coupling is obtained from the $R_1 \rightarrow D^* \bar{K}$ width.

$$\frac{d\Gamma}{dM_{\text{inv}}(D^{*+} K^-)} = \frac{1}{(2\pi)^3} \frac{1}{4M_{\bar{B}^0}^2} p_{\bar{D}^{*0}} \tilde{p}_{K^-} \sum |t'|^2 \quad (6)$$

$$\text{where } \tilde{p}_{K^-} = \frac{\lambda^{1/2}(M_{\text{inv}}^2(D^{*+} K^-), m_{D^*}^2, m_K^2)}{2M_{\text{inv}}(D^{*+} K^-)}, p_{\bar{D}^{*0}} = \frac{\lambda^{1/2}(M_{\bar{B}^0}^2, m_{\bar{D}^{*0}}^2, M_{\text{inv}}^2(D^{*+} K^-))}{2M_{\bar{B}^0}}.$$

Background for $\bar{B}^0 \rightarrow \bar{D}^{*0} D^{*+} K^- \quad -it = -iC\epsilon(D^{*0}) \cdot \epsilon(D^{*+})$

$$\frac{d\Gamma_{\text{bac}}}{dM_{\text{inv}}(D^{*+} K^-)} = \frac{1}{(2\pi)^3} \frac{1}{4M_{\bar{B}^0}^2} p_{\bar{D}^{*0}} \tilde{p}_{\bar{K}} 3 C^2 \quad (7)$$

How can we observe the $J^P = 1^+$ state?

Dai, Molina and Oset, PLB 832 (2022)

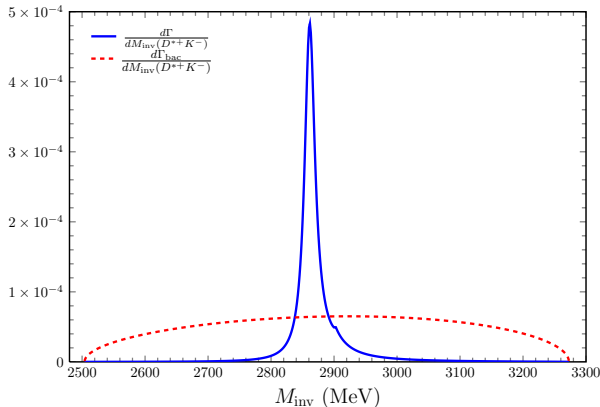


Figure 6: $\frac{d\Gamma}{dM_{\text{inv}}}$ for the R_1 production versus the background, $\frac{d\Gamma_{\text{bac}}}{dM_{\text{inv}}}$, in the $\bar{B}^0 \rightarrow \bar{D}^{*0} D^{*+} K^{*-}$ reaction in a global arbitrary normalization. M_{inv} is the invariant mass of $D^{*+} K^-$. $\mathcal{B}_R(R_1; R_1 \rightarrow D^{*+} K^-) = 4.24 \times 10^{-3}$.

How can we observe the $J^P = 1^+$ state?

Similar results for the $\bar{B}^0 \rightarrow D^{*+} K^{*-} K^{*0} \rightarrow R_1 K^{*0} \rightarrow D^{*+} K^- K^{*0}$ process. [Dai, Molina and Oset, PRD105 \(2022\)](#)

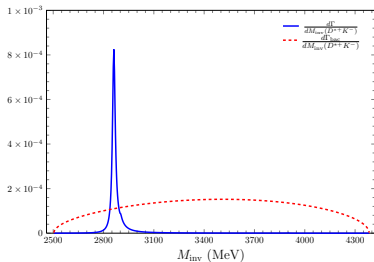


Figure 7: $\frac{d\Gamma}{dM_{\text{inv}}}$ for R_1 production and $\frac{d\Gamma_{\text{bac}}}{dM_{\text{inv}}}$ for background in the $\bar{B}^0 \rightarrow K^{*0} D^{*+} K^-$ reaction in global arbitrary units versus the $D^{*+} K^-$ invariant mass.

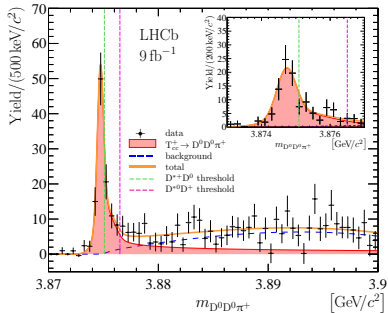
The $X_0(2866)$ can also be seen in:

$\bar{B}^0 \rightarrow K^0 D^{*+} K^{*-} \rightarrow K^0 X_0 \rightarrow K^0 D^+ K^-$ [Dai, Molina, Oset, PRD105, 2022](#)

$B^- \rightarrow D^- D^{*+} K^{*-} \rightarrow D^- X_0 \rightarrow D^- D^+ K^-$ [PLB 832, 2022](#)

Doubly-charmed states

T_{cc}^+ signal in $D^0 D^0 \pi^+$

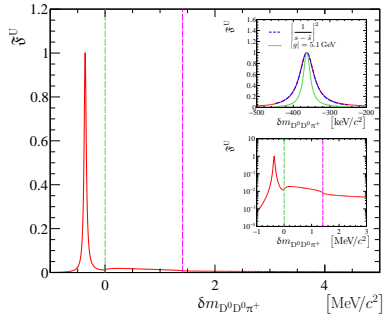


Nature 2022. Spectra without correction by experimental resolution:

$$m_{\text{exp}} = 3875.09 \text{ MeV} + \delta m_{\text{exp}}$$

$$\delta m_{\text{exp}} = -273 \pm 61 \pm 5^{+11}_{-14} \text{ keV};$$

$$\Gamma = 410 \pm 165 \pm 43^{+18}_{-38} \text{ keV}$$



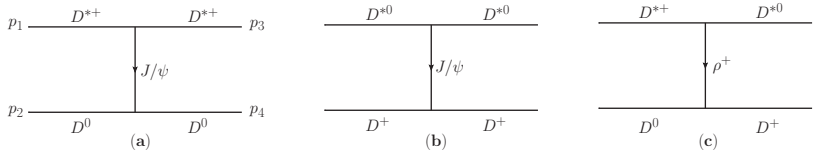
Nature 2022. Spectra corrected by experimental resolution and analyzed with a three-body unitary amplitude

$$\delta m_{\text{exp}} = -360 \pm 40^{+4}_{-0} \text{ keV};$$

$$\Gamma = 48 \pm 2^{+0}_{-14} \text{ keV}$$

Remarkably close to the $D^{*+} D^0 / D^{*0} D^+$ thresholds!

T_{cc}^+ signal in $D^0 D^0 \pi^+$



Feijoo, Liang, Oset, PRD104 (2021)

$$T = [1 - VG]^{-1}; \quad V_{ij} = C_{ij} g^2 (p_1 + p_3) \cdot (p_2 + p_4) \vec{\epsilon} \cdot \vec{\epsilon}; \quad C_{ij} = \begin{pmatrix} \frac{1}{M_{J/\psi}^2} & \frac{1}{m_\rho^2} \\ \frac{1}{m_\rho^2} & \frac{1}{M_{J/\psi}^2} \end{pmatrix}.$$

Individually the $D^{*+}D^0$, $D^{*0}D^+$ states have a weak and repulsive interaction, but the isospin combinations,

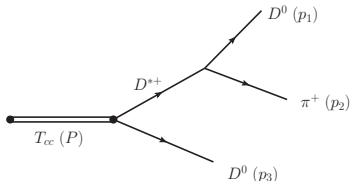
$$|D^*D, I = 0\rangle = -\frac{1}{\sqrt{2}}(D^{*+}D^0 - D^{*0}D^+), \quad (8)$$

$$|D^*D, I = 1, I_3 = 0\rangle = -\frac{1}{\sqrt{2}}(D^{*+}D^0 + D^{*0}D^+), \quad (9)$$

$$C_{00} = \frac{1}{M_{J/\psi}^2} - \frac{1}{m_\rho^2}; \quad C_{11} = \frac{1}{M_{J/\psi}^2} + \frac{1}{m_\rho^2}; \quad C_{01} = 0; \quad (10)$$

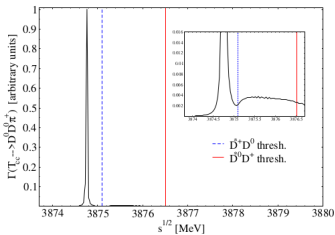
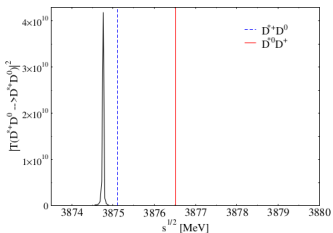
lead to an attraction in $I = 0$ and repulsion in $I = 1$.

T_{cc}^+ signal in $D^0 D^0 \pi^+$

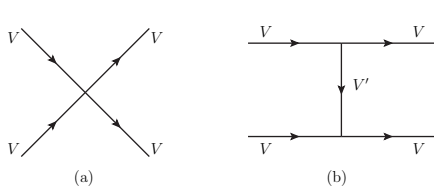


$$\frac{d\Gamma}{dM_{12}^2 dM_{23}^2} = \frac{1}{2} \frac{1}{(2\pi)^3} \frac{1}{s^{3/2}} |t|^2,$$

$$\implies \Gamma = 43 \text{ KeV}$$



Works about the T_{cc}^+ : Feijoo, Liang, Oset, PRD104 (2021); M. Albaladejo, PLB (2021); Meng-Lin Du, Baru, Dong, Filin, Feng-Kun Guo, Hanhart, Nefediev, Nieves, Qian Wang PRD105(2022); Xiang-Kun Dong, Feng-Kun Guo, Bing-Song Zou, Com.Theo.Phys. 73 (2021)...



$$\mathcal{L}_{III}^{(c)} = \frac{g^2}{2} \langle V_\mu V_\nu V^\mu V^\nu - V_\nu V_\mu V^\mu V^\nu \rangle$$

$$\mathcal{L}_{III}^{(3V)} = ig \langle [V_\mu, \partial_\nu V_\mu] V^\nu \rangle$$

Repulsion for $I = 1$

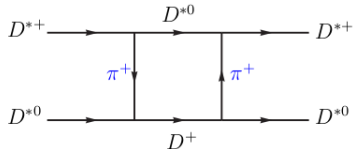
J	Amplitude	Contact	V-exchange	\sim Total
0	$D^*D^* \rightarrow D^*D^*$	0	0	0
1	$D^*D^* \rightarrow D^*D^*$	$0 \frac{g^2}{4} \left(\frac{2}{m_{J/\psi}^2} + \frac{1}{m_\omega^2} - \frac{3}{m_\rho^2} \right) \{(p_1 + p_3).(p_2 + p_4) + (p_1 + p_4).(p_2 + p_3)\}$	$-25.4g^2$	$-25.4g^2$
2	$D^*D^* \rightarrow D^*D^*$	0	0	0

Table 5: Tree level amplitudes for D^*D^* in $I = 0, C = 2, S = 0$.

J	Amplitude	Contact	V-exchange	\sim Total
0	$D_s^*D^* \rightarrow D_s^*D^*$	$-4g^2$	$\frac{g^2(p_1+p_4)(p_2+p_3)}{m_{K^*}^2} + \frac{g^2(p_1+p_3)(p_2+p_4)}{m_{J/\psi}^2}$	$19g^2$
1	$D_s^*D^* \rightarrow D_s^*D^*$	0	$-\frac{g^2(p_1+p_4)(p_2+p_3)}{m_{K^*}^2} + \frac{g^2(p_1+p_3)(p_2+p_4)}{m_{J/\psi}^2}$	$-19.5g^2$
2	$D_s^*D^* \rightarrow D_s^*D^*$	$2g^2$	$\frac{g^2(p_1+p_4)(p_2+p_3)}{m_{K^*}^2} + \frac{g^2(p_1+p_3)(p_2+p_4)}{m_{J/\psi}^2}$	$25.0g^2$

Table 6: Tree level amplitudes for $D^*D_s^*$ in $I = 1/2, C = 2, S = 1$.

T_{cc} states from $D^*D^*/D^*D_s^*$



$$\mathcal{L}_{VPP} = -ig \langle [P, \partial_\mu P] V^\mu \rangle$$

$$\mathcal{L}_{VVP} = \frac{G'}{\sqrt{2}} \epsilon^{\mu\nu\alpha\beta} \langle \partial_\mu V_\nu \partial_\alpha V_\beta P \rangle$$

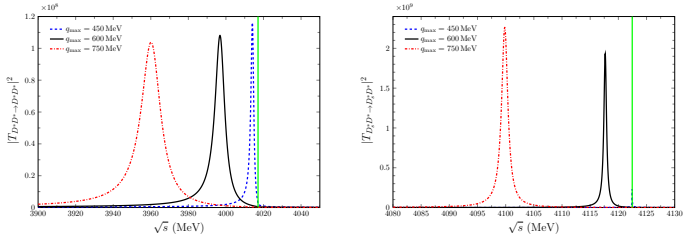
$$G' = \frac{3g'}{4\pi^2 f}; \quad g' = -\frac{G_V m_\rho}{\sqrt{2} f^2}$$

$$\begin{aligned} -i t &= 4 \frac{9}{2} \frac{1}{3} \int \frac{d^4 q}{(2\pi)^4} \frac{1}{2E_{D^*}(\mathbf{q})} \frac{i}{p_1^0 - q^0 - E_{D^*}(\mathbf{q}) + i\epsilon} \frac{1}{2E_D(\mathbf{q})} \\ &\times \frac{i}{p_2^0 + q^0 - E_D(\mathbf{q}) + i\epsilon} \frac{i}{q^2 - m_\pi^2 + i\epsilon} \frac{i}{(p_2 - p_4 + q)^2 - m_\pi^2 + i\epsilon} \mathbf{q}^4 \end{aligned}$$

$$\begin{aligned} Im V_{\text{box}} &= -\frac{6}{8\pi\sqrt{s}} q^5 E_{D^*}^2 (\sqrt{2}g)^2 \left(\frac{G'}{2}\right)^2 \left(\frac{1}{(p_2^0 - E_D(\mathbf{q}))^2 - \mathbf{q}^2 - m_\pi^2}\right)^2 F^4(q) F_{HQ} \\ q &= \frac{\lambda^{1/2}(s, m_{D^*}^2, m_D^2)}{2\sqrt{s}}; \quad E_{D^*} = \frac{\sqrt{s}}{2}; \quad F(q) = e^{q^2/\Lambda^2} \end{aligned}$$

T_{cc} states from $D^*D^*/D^*D_s^*$

$$q^0 = p_1^0 - E_{D^*}(q); \quad F_{HQ} = \left(\frac{m_{D^*}}{m_{K^*}} \right)^2; \quad V \rightarrow V + i \operatorname{Im} V_{\text{box}}$$



$q_{\max} = 450$ MeV	$q_{\max} = 420$ MeV
$M_{D^*D^*}$	4014.08 MeV
$B_{D^*D^*}$	3.23 MeV
$\Gamma_{D^*D^*}$	2.3 MeV
$M_{D_s^*D^*}$	4122.46 MeV (cusp)
$\Gamma_{D_s^*D^*}$	70 – 100 KeV

Extension Weinberg compositeness condition, Gamermann, Nieves, Oset, Arriola, PRD81 (2010), Toki, Garcia-Recio, Nieves, PRD77 (2008)

Z_{cs} states

Hidden-charm strange state

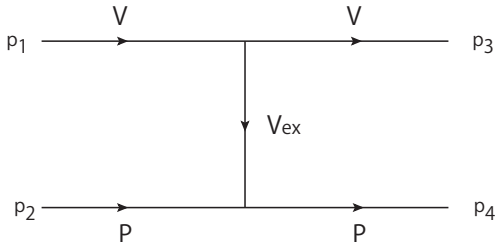
BESIII (2020) has reported a state, $Z_{cs}(3985)$, from the $D_s^{*-}D^0$, $D_s^-D^{*0}$ invariant mass distribution of $e^+e^- \rightarrow K^+(D_s^{*-}D^0 + D_s^-D^{*0})$.

$$M = 3982.5^{+1.8}_{-2.6} \pm 2.1 \text{ MeV}, \quad \Gamma = 12.8^{+5.3}_{-4.4} \pm 3.0 \text{ MeV}. \quad (11)$$

7 MeV above the $D_s^{*-}D^0$, $D_s^-D^{*0}$ threshold. SU(3) partner of the $Z_c(3900)$ state?, changing u or d by an s quark.

Hidden-Gauge Formalism Ikeno,Molina,Oset, PLB814(2021)

Channels : $J/\psi K^-$ (1), $K^{*-}\eta_c$ (2), $D_s^{*-}D^0$ (3), $D_s^-D^{*0}$ (4)



Hidden-charm strange state

$$V_{ij} = C_{ij} g^2 (p_2 + p_4)(p_1 + p_3); \quad \bar{m}_D = 1916 \text{ MeV}, \bar{m}_{D^*} = 2060 \text{ MeV}$$

$$C_{ij} = \begin{pmatrix} 0 & 0 & \frac{1}{m_{D^*}^2} & \frac{1}{m_{D_s^*}^2} \\ 0 & \frac{1}{m_{D_s^*}^2} & \frac{1}{m_{D^*}^2} & -\frac{1}{m_{J/\psi}^2} \\ -\frac{1}{m_{J/\psi}^2} & 0 & -\frac{1}{m_{J/\psi}^2} & \end{pmatrix},$$

and the product $\vec{\epsilon} \cdot \vec{\epsilon}'$ has been omitted. We build the combinations:

$$A = \frac{1}{\sqrt{2}}(D_s^- D^{*0} + D_s^{*-} D^0), \quad B = \frac{1}{\sqrt{2}}(D_s^- D^{*0} - D_s^{*-} D^0).$$

Combination A couples to $J/\psi K^-$, $K^{*-} \eta_c$, while B not.

$$J/\psi K^- \text{ (1)}, \quad K^{*-} \eta_c \text{ (2)}, \quad \frac{1}{\sqrt{2}}(D_s^- D^{*0} + D_s^{*-} D^0) \text{ (3)}$$

Similar to $Z_c(3900)$, $\bar{D}^* D + \bar{D} D^*$, $G = +$, **Aceti, Bayar, Oset, Martinez Torres, Khemchandani, Navarra, Dias, Nielsen PR90 (2014)**

Hidden-charm strange state: $e^+e^- \rightarrow K^+(D_s^{*-}D^0 + D_s^-D^{*0})$

$$V_{ij} = g^2 C_{ij} \frac{1}{2} \left[3M_{12}^2 - (m_1^2 + m_2^2 + m_3^2 + m_4^2) - \frac{1}{M_{12}^2} (m_1^2 - m_2^2)(m_3^2 - m_4^2) \right],$$

where $M_{12}^2 = (p_1 + p_2)^2$. q^2 correction in the propagators: $q^2 = 0$ for V_{ii} and $q^2 = M^2 + M_{D^*}^2 - 2EM_{D^*}^2$, for V_{13}, V_{23} , with $E = \frac{M_{12}^2 + M^2 - m^2}{2M_{12}}$.

$$C_{ij} = \begin{pmatrix} 0 & 0 & \frac{\sqrt{2}}{\bar{m}_{D^*}^2} \\ & 0 & \frac{\sqrt{2}}{\bar{m}_{D^*}^2} \\ & & -\frac{1}{m_{J/\psi}^2} \end{pmatrix}.$$

$$T = [1 - VG]^{-1} V,$$

$$G_I = \int \frac{d^3 q}{(2\pi)^3} \frac{\omega_1 + \omega_2}{2\omega_1\omega_2} \frac{1}{(P^0)^2 - (\omega_1 + \omega_2)^2 + i\epsilon}$$

$$\omega_1 = \sqrt{m^2 + \vec{q}^2}, \omega_2 = \sqrt{M^2 + \vec{q}^2}, \text{ and } |\vec{q}| < q_{\max}. q_{\max} \sim 700\text{--}850 \text{ MeV in Ajeti,Oset, PRD90(2014) BS factor, } \psi = -\frac{1}{3} + \frac{4}{3} \left(\frac{m_L}{m_H} \right)^2 \quad (2.8)$$

$$p = \frac{\lambda^{1/2}(s, m_K^2, M_{D_s D^*}^2)}{2\sqrt{s}},$$

$$\tilde{q} = \frac{\lambda^{1/2}(M_{D_s D^*}^2, m_{D_s}^2, m_{D^*}^2)}{2M_{D_s D^*}},$$

$$\frac{d\sigma}{dM_{\bar{D}_s D^*}} = \frac{1}{s\sqrt{s}} p \tilde{q} N |T_{33}|^2$$

Hidden-charm strange state: $e^+e^- \rightarrow K^+(D_s^{*-}D^0 + D_s^-D^{*0})$

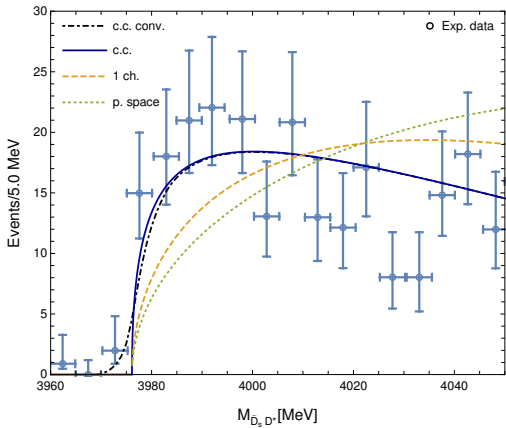


Figure 8: Results of $d\sigma/dM_{\bar{D}_s D^*}$. Solid line: Result for the $\bar{D}_s D^* + \bar{D}_s^* D$ combination with its coupled channels (c.c.). Dashed line: Result for the single channel $\bar{D}_s D^* - \bar{D}_s^* D$ combination (1 ch.). Dotted line: phase space. Dashed-dotted line: result folded with the experimental resolution (c.c. conv.).

Are there Z_{cs} states from $D_s^* \bar{D}^*$?

Ikeno, Molina and Oset, PRD105(2022) Channels: $D_s^{*+} \bar{D}^{*0}$, $J/\psi K^{*+}$

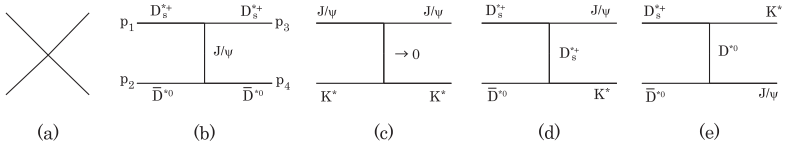
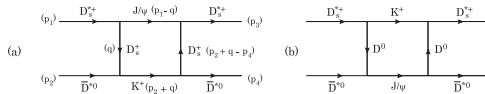
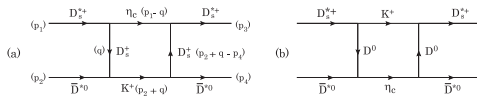


Figure 9: Contact term (a) and vector exchange terms (b, c, d, e) involved in the interaction of the coupled channels.

$\eta_c K^+$, $J/\psi K^+$ included via box diagrams:



Are there Z_{cs} states from $D_s^* \bar{D}^*$?

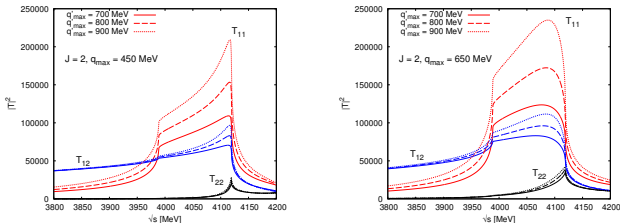


Figure 10: $|T|^2$ for each channel are shown for $J = 2$ and the different q'_max value of the $J/\psi K^*$ channel. The value of $q_\text{max} = 450, 650$ MeV is fixed for the $D_s^* \bar{D}^*$ channel.

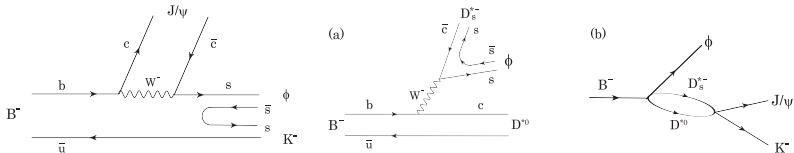


Figure 11: Left: Mechanism for $B^- \rightarrow J/\psi \phi K^-$ decay based on internal emission. Center: External emission and right, decay into $J/\psi K^-$.

Are there Z_{cs} states from $D_s^* \bar{D}^*$?

Invariant mass distribution for $B^- \rightarrow J/\psi \phi K^-$

$$\frac{d\Gamma}{dM_{\text{inv}}(J/\psi K)} = \frac{1}{(2\pi)^3} \frac{1}{4M_B^2} p_\phi \tilde{p}_K |t|^2 \quad (12)$$

with $p_\phi = \frac{\lambda^{1/2}(M_B^2, M_\phi^2, M_{\text{inv}}^2(J/\psi K))}{2M_B}$, $\tilde{p}_K = \frac{\lambda^{1/2}(M_{\text{inv}}^2(J/\psi K), M_{J/\psi}^2, M_K^2)}{2M_{\text{inv}}(J/\psi K)}$

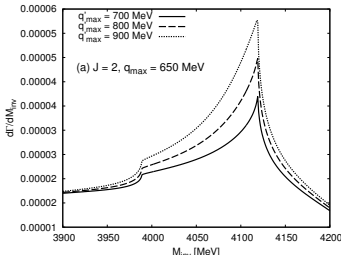
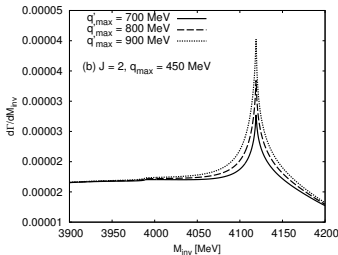
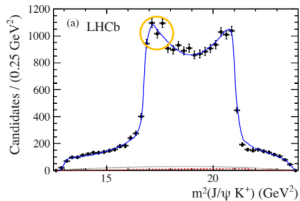
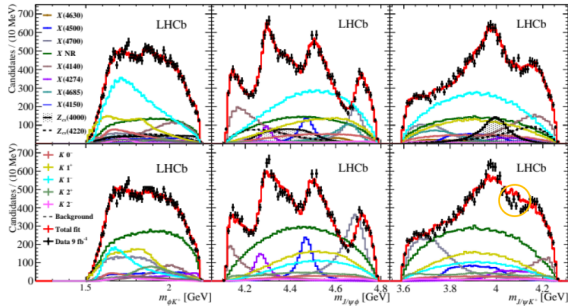


Figure 12: The mass distribution for $B^- \rightarrow J/\psi \phi K^-$ is shown as a function of $M_{\text{inv}}(J/\psi K)$. (a) $q_{\text{max}} = 650$ MeV and (b) $q_{\text{max}} = 450$ MeV are fixed for the $D_s^* \bar{D}^*$ channel and the different values of q'_max for the $J/\psi K^*$ channel are used as shown in the figure. The result corresponds to the case of $J = 2$ for $D_s^* D^{*0}$.

Are there Z_{cs} states from $D_s^* \bar{D}^*$?

$B^+ \rightarrow J/\psi \phi K^+$, LHCb, PRL127(2021)



$\bar{B}^0 \rightarrow J/\psi K^- K^+$, LHCb,
PRD87(2013)

Conclusions

Conclusions

- The $X_0(2866)$ and $T_{cc}(3875)$ are good candidates to be $D^*\bar{K}^*$ and DD^* molecular states respectively
- We have made predictions on D^*D^* states for $I = 0, J^P = 1^+$
- We have proposed several reactions where the $J = 1^+$ state (partner of the X_0) can be observed
- The $Z_{cs}(3985)$ can be explained as a threshold effect from the coupled-channel interaction
- There can be also another cusp corresponding to the $D_s^*\bar{D}^*$ interaction with $J/\psi K^*$, and we suggest to look around 4120 MeV in the data of the B decays